

# Recovery of Relaxation and Retardation Spectra over Expanded Intervals with Increased Density of Spectrum Points

VAIRIS SHTRAUSS  
 Institute of Polymer Mechanics  
 University of Latvia  
 23 Aizkraukles Street, LV 1006 Riga  
 LATVIA  
[strauss@pmi.lv](mailto:strauss@pmi.lv)

*Abstract:* - Asymmetric filtering algorithms with the shifted origins (zero points) of impulse responses are proposed to use for expanding time intervals of the relaxation and retardation spectra (RRS) and increasing density of spectrum points. A filter bank is presented recovering RRS from the real part of complex compliance recorded at frequencies spaced geometrically with progression ratio 2, which produces the spectrum points with doubled density over the retardation time interval 4 times exceeding the reciprocal frequency range.

*Key-Words:* - Relaxation and Retardation Spectrum (RRS), Geometric Sampling, Symmetric and Asymmetric RRS Recovery Filters, Filter Bank

## 1 Introduction

Relaxation and retardation spectrum (RRS) is one of the most fundamental quantities in linear theory of viscoelasticity [1-4] and other relaxation theories [4-6]. RRS is independent of loading (excitation) and is used in various studies, such as examination of the relationship between the molecular weight distribution and properties of a material, prediction of the behaviour of materials after an arbitrary excitation, interconversion of material functions, etc.

Approaches used for RRS determination can be classified as *parametric* and *non-parametric* [7,8]. The parametric approach presumes an *a priori* model form for the material behaviour and RRS is determined by parametric curve fitting techniques. Contrary, no any assumption is made about the material behaviour in the non-parametric approach, where RRS is determined by numerical inversion of the integral transforms interconnecting the material responses with the spectrum. These inversions are known to be severely ill-posed resulting in unstable solutions, where small perturbations in the input data (noise) can yield unrealistic high perturbations in the spectra.

Based on the advanced signal processing concepts [9,10], a non-parametric, computationally efficient *functional filtering* approach [11] has been recently developed for a wide class of interconversions between linear rheologic and viscoelastic material functions, including also RRS recovery. The approach treats an interconversion problem as a linear filtering (convolution) task on the logarithmic frequency (time) scale and suggests to solve it by the appropriate

discrete-time filter processing geometrically<sup>1</sup> sampled data

$$\omega_n = \omega_0 q^n, \quad n = 0, \pm 1, \pm 2, \dots, \quad q > 1, \quad (1)$$

where  $q$  is progression ratio specifying the sampling rate in the sense that  $\ln q$  specifies the distance between samples on logarithmic scale, i.e. plays formally a role of sampling period, whereas its reciprocal describes the appropriate sampling frequency.

In the functional filtering context [12,13], RRS recovery relates to severely ill-posed linear inverse (deconvolution) problem, where the ill-posedness of the problem and the ill-conditionness of the algorithms manifest as extremely high noise amplification. Based on learning and controlling noise amplification by varying sampling rate (progression ratio  $q$ ), a method [14-16] has been developed for designing deconvolution filters with the desired noise gains producing maximum accurate output signals.

The filtering algorithms, although computational efficient, accurate and have be constructed with prescribed noise amplification [14], are not free from some drawbacks, which limit their usage, and particularly implementation in measuring systems [17].

And so, RRS recovery filters, as all discrete convolution algorithms [9], suffer from of so-called *end effect* problem [10], appearing as shortening usable filtered sequences. Due to the geometric

<sup>1</sup> *Logarithmic sampling* and *exponential sampling* are also used in literature for arrangement (1)

sampling (1), relaxation/retardation time intervals reduces exponentially, and, comparing to the frequency (time) ranges of input functions, reaches shortenings of hundreds and more times in practice.

Next, to keep noise amplification at acceptably low level, relatively high progression ratios  $q=2.4-4.2$  must be used [13] resulting in relatively rare spectrum points and, therefore, poor resolution. In addition, non-integer – finite decimal progression ratios are not practical and require resampling input data.

The presented paper focuses on elimination of the mentioned drawbacks of filtering algorithms used for RRS recovery.

## 2 RRS Recovery by Filtering Algorithms

To determine the spectrum, a RRS recovery filter convolves samples of geometrically sampled material function with filter's impulse response. In [12,13], three basic algorithms have been derived for calculation of RRS from the eight material functions. For example, the algorithm for RRS recovery from the real and imaginary parts of dynamic material functions can be presented in the following form:

$$F(\tau) = \sum_{n=-(N-1)/2}^{(N-1)/2} h[n] x\left(\frac{1}{\tau} q^{-n}\right) \quad (2)$$

where  $F(\tau)$  is relaxation or retardation spectrum,  $x(\cdot)$  is a dynamic material function,  $h[n]$  is the impulse response (IR) containing  $N$  non-zero coefficients. In the case of odd number  $N$  of coefficients, integer indexes  $n$  are used in Eq. (2), while  $n$  becomes halves of odd numbers for even number  $N$  of coefficients. Filtering algorithm (2) is symmetric with the origin (zero point) of IR located in its geometric centre and having an equal number of coefficients ( $N/2$  for even  $N$  and  $(N-1)/2$  for odd  $N$ ) about the origin with negative and positive indices.

The same coefficients  $h[n]$  are used for recovery of the relaxation and retardation spectrum from the imaginary parts of dynamic material functions [12,13], however, the coefficients differ by signs for calculation of the relaxation spectrum from the real part of modulus and the retardation spectrum from the real part of compliance function.

Algorithm (2) multiplies a set of geometrically sampled  $N$  samples of a material function  $x(\omega_0 q^n)$  (samples 3 – 8, in Fig. 1) by the reversed filter coefficients  $h[n]$  and adds the products. The origin of IR is centred at the position on the frequency axis corresponding to the reciprocal of the

relaxation/retardation time  $\omega_0 = 1/\tau$ , at which the spectrum is calculated. For IR with 6 coefficients shown in Fig. 1, this position coincides with the geometric mean of the frequencies for samples 5 and 6. A RRS recovery filter is *sliding* or *moving* one, depending on descending or ascending order of the relaxation/retardation times chosen to calculate the spectrum, it moves one sample to the left or right and repeats processing to produce next spectrum value.

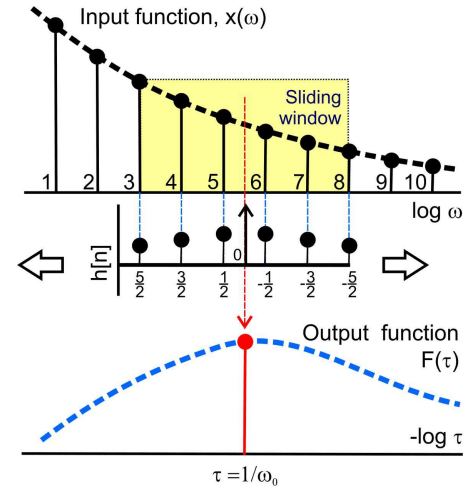


Fig. 1. Illustration of calculating a spectrum value by a 6-point RRS recovery filter.

Algorithm (2) may be used for input sequences sampled geometrically with the rate increased by an integer factor of  $L$ , i.e. for the data sampled at the ratio  $q^{1/L}$ . Then the filter must process every  $L$ -th input sample, however, it should move one sample to the left or right to calculate next spectrum value, therefore, producing the spectrum points with the sampling density equal to that of input data.

It has been demonstrated [12,13] that at least two performance parameters – *accuracy* and *noise amplification*, conflicting with one another, shall be controlled for RRS recovery filters. Following the suggestion in [14,15], mean squared error between calculated spectrum  $\hat{F}(\tau_m)$  and exact spectrum  $F(\tau_m)$

$$E = (1/K) \sum_{m=1}^K [\hat{F}(\tau_m) - F(\tau_m)]^2 \quad (3)$$

will be used here as an accuracy measure. As a reference spectrum,  $F(\tau)$  corresponding to the Cole-Cole (CC) relaxation model [18] will be used in Eq. (3) with  $\alpha = 0.7$  and  $\tau_0 = 1$ , calculated for  $M = 100$  equally spaced time points on a logarithmic scale within the range  $10^{-3} \leq \tau \leq 10^3$ .

In its turn, noise amplification will be measured by noise gain (amplification coefficient) [14,15]

$$S = \sum_n h^2[n] \quad (4)$$

showing how the noise variance  $\sigma_x^2$  of input data is transmitted to the noise variance  $\sigma_F^2$  of the spectrum  $S = \sigma_F^2 / \sigma_x^2$ .

### 3 Asymmetric Algorithms

In the sliding filtering mode (see the previous Section), a value of the relaxation/retardation time is varied by moving an IR along the input sequence discretely. Apart from this traditional mode, one more way is to alter the relaxation/retardation time by moving the origin of a standing (fixed) IR. In practice, this mode may be implemented by processing a fixed set of  $N$  input samples by multiple filters, whose origins of IRs are shifted according to the desired alteration of relaxation/retardation time.

In this multiple filtering mode, IRs become asymmetric against their origins and the algorithm of a separate filter may be described by an expression

$$F(\tau) = \sum_{n=-(N-1)/2-s}^{(N-1)/2-s} h(n)x\left(\frac{1}{\tau}q^{-n}\right), \quad (5)$$

where  $s$  is the shift of the origin of IR. Filters with  $s \neq 0$  will be qualified further as asymmetric ones.

The advantage of asymmetric filters is a possibility to determine multiple spectrum values from the same set of  $N$  input samples. This allows to employ asymmetric filters for increasing density of spectrum points, as well as, to compensate shortening relaxation/retardation time intervals due to the end effects.

Asymmetric filters have been used to expand output sequence in converting the statistic material functions into the dynamic ones, and vice versa [20], as well as in calculating the imaginary part of dynamic material functions from the real part [21]. Experience gained with these interconversions has showed that, in general, the performance of the asymmetric filters deteriorates with increasing the shift of the origin, however, the intervals for output functions to be approximately equal to those of input data can be attained to keep acceptable performance.

#### 3.1 Increase of Density of Spectrum Points

Processing of a fixed set of  $N$  input samples in turn by  $L$  filters, whose origins of IRs are shifted from each other by a distance  $1/L$ , produces  $L$  spectrum

points located from each other by time  $q^{1/L}$ . Combining such  $L$  filters in an array and calculating the spectrum by sliding the array along the input sequence, will increase the density of the spectrum points by an integer factor of  $L$  to compare with the density of input samples.

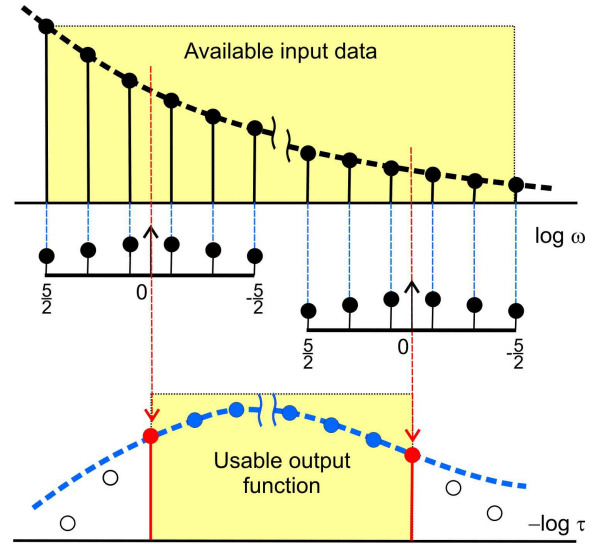


Fig. 2. Ultimate alignments of IR to an input sequence and a usable output sequence for a symmetric 6-point filter. Open circles are the unusable spectrum points calculated from incomplete information containing zeros.

#### 3.2 Expansion of Time Intervals

Algorithm (1) and (5) produces a spectrum value correctly only if all  $N$  input samples without zeros are involved in calculation. Since the origin of IR specifying a value of relaxation/retardation time is normally located in the vicinity of IR midpoint, input samples are required at the both ends of input sequence for aligning IR to calculate spectrum points correctly from all the  $N$  input samples (Fig. 2). With such IR alignment, a usable output sequence shortens at the both – left and right ends by a total reduction of  $N-1$  samples to compare with the input sequence. This shortening is particularly undesirable for geometrically sampled datasets, because reduces relaxation/retardation time interval  $\tau_{\max} / \tau_{\min}$  exponentially – by  $q^{N-1}$  times to compare with frequency range  $\omega_{\max} / \omega_{\min}$  of input function. It should be remembered that elongation of filter length  $N$ , resulting normally in the higher accuracy, will shorten range  $\tau_{\max} / \tau_{\min}$ .

Usually, the shortening output sequences due to the end effects is compensated by artificial extension

of the original data at the both ends by extrapolation [19] and placement of the end effects out of range of the available input data. However, the extrapolation is not in compliance with the philosophy of non-parametric model-free interconversion of material functions [11] when data transformations are implemented without preliminary assumptions about the behaviour of the material and its responses.

As it is seen from Fig. 2, the output sequence formed from the low frequency data can be prolonged by processing the first  $N$  input samples by asymmetric filters, whose origins of the reversed IR are shifted the left ( $s > 0$ , e.g.,  $s = 1, 2, \dots$ ). These asymmetric filters contain decreased number of positively indexed coefficients and increased number of negatively indexed coefficients. Similarly, the output sequence formed from the high frequency data can be prolonged by processing the last  $N$  input samples by filters, whose origins are shifted the right ( $s < 0$ , e.g.,  $s = -1, -2, \dots$ ) having decreased number of negatively indexed coefficients and increased number of positively indexed coefficients.

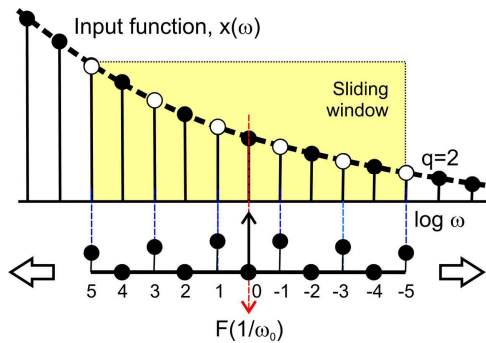


Fig. 3. IR of a 6-point filter adapted for processing data sampled at doubled sampling rate. Every other input sample (open circles) makes a contribution in the spectrum point.

### 4 Filter Bank

To overcome the inherent drawbacks of the filtering algorithms (shortening intervals of relaxation/retardation time, rare spectrum points, inconvenience of finite decimal (non-integer) progression ratios), we had set a target to construct a RRS recovery algorithm that in addition to high accuracy and acceptably low noise amplification would allow to process data recorded at geometrically spaced frequencies with progression ratio  $q = 2$ , typically used in interconversions between material functions [11], and to produce the spectrum points with doubled density with  $q = \sqrt{2} = 1.414$  over the time intervals as expanded as possible.

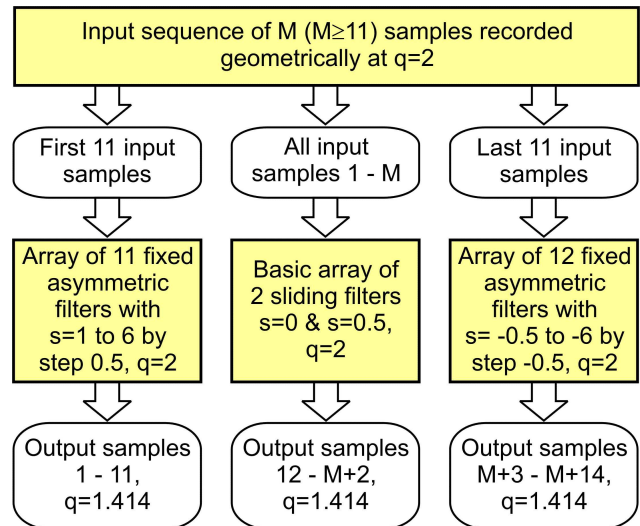


Fig. 4. Structure of the filter bank.

The algorithm was formed as a filter bank composed of 6-point filters operating at  $q = 4$ . This progression ratio was chosen in order to provide a trade-off between accuracy, noise amplification and a possibility of adjusting the filter to process data sampled with doubled sampling rate. To adapt the filters to process data sampled at  $q = 2$ , zero coefficients were inserted between every other coefficient of IR (Fig. 3) modifying a 6-point filter operating at  $q = 4$  into an 11-point filter operating at  $q = 2$ . Since multiplication of input samples by zero coefficients gives zero products, the filter processes every other input sample, and according to Eq. (4) retains original low noise gain corresponding to  $q = 4$ .

The structure of the bank is shown in Fig. 3. The bank was composed of 25 filters whose coefficients  $h[n]$  were found by the method [14,15]. The filters were integrated in 3 arrays:

- (i) a basic array composed of a sliding symmetric filter ( $s = 0$ ) and an sliding asymmetric filter ( $s = 0.5$ ),
- (ii) an array for processing the first 11 input samples composed of 11 fixed asymmetric filters, whose origins are shifted positively with  $s = 1$  to 6 by step 0.5,
- (iii) an array for processing the last 11 input samples composed of 12 fixed asymmetric filters, whose origins are shifted negatively with  $s = -0.5$  to -6 by step -0.5.

The filter bank is applicable for input sequences of  $M = 11$  samples and longer and it produces the spectrum sequences consisting from  $M + 14$  samples.

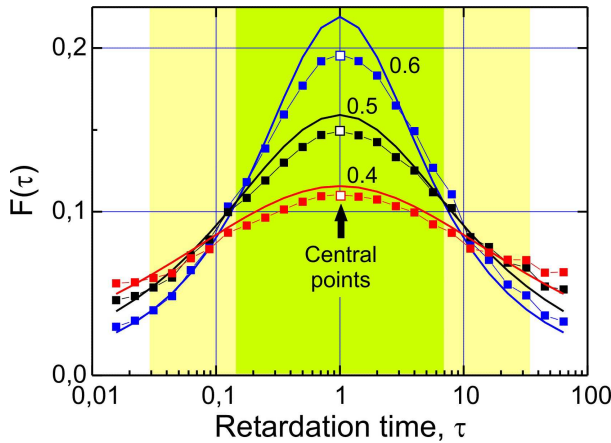


Fig. 5. Retardation spectrum recovered from the real part of complex compliance corresponding to CC model with different values of parameter  $\alpha$  (numbers near the curves). Solid lines – exact spectrum.

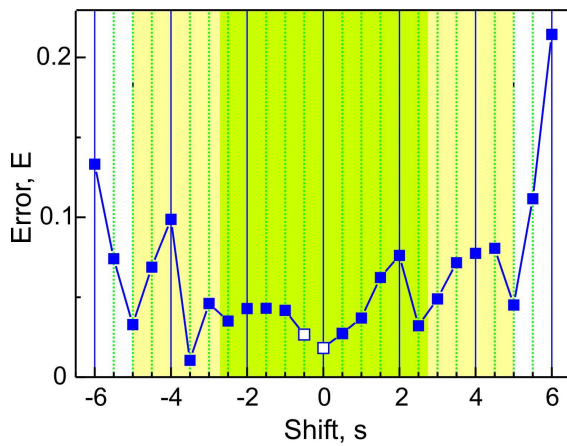


Fig. 6. Error  $E$  of the filters of the bank. Open squares correspond to the sliding filters.

## 5 Performance evaluation

Fig. 5 shows the spectrum recovered by the bank from 11 input samples occupying frequency range  $\omega_{\max}/\omega_{\min} = 1024$ . In this case, each of 25 spectrum points is calculated by a separate filter. If, in the normal sliding filtering mode, only central points (open squares) can be obtained by the sliding symmetric filter with  $s=0$ , then integration of the filters into the bank allows to recover the spectrum with the doubled density over the retardation time interval  $\tau_{\max}/\tau_{\min} = 4096$ , or, in general, over the interval  $0.5\omega_{\max}^{-1} < \tau < 2\omega_{\min}^{-1}$ , which 4 times exceeds the reciprocal frequency range  $\omega_{\max}^{-1} < \tau < \omega_{\min}^{-1}$  (pale shaded area in Fig. 5) and 92.6 times – the interval  $\omega_{\max}^{-1}e^{\pi/2} < \tau < \omega_{\min}^{-1}e^{-\pi/2}$  predicted by so-called sampling localization theorem [22] (the darker shaded area).

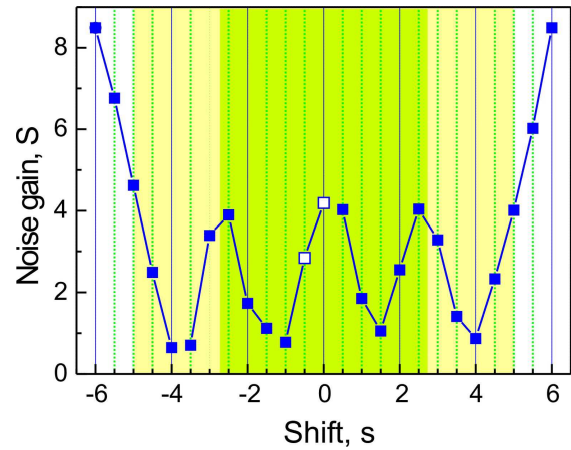


Fig. 7. Noise gain  $S$  of the filters of the bank. Open squares correspond to the sliding filters.

It is worth paying particular attention to the fact that the first 2 and last 2 spectrum points (see Fig. 5) are located outside the reciprocal frequency range of 11 input samples involved in calculation. A possibility to determine such points has been theoretically justified in [23], where it has been proved that the relaxation spectrum can in principle be recovered from the data limited to any range, however short and wherever located. Therefore, the results obtained here give some experimental evidence in the part of the proof that the relaxation spectrum can be recovered from the data “limited to any range, wherever located”.

In Fig. 6, error (3) is shown for the filters of the bank as a function of the shift of the origins of IRs, while Fig. 6 illustrates noise gains (4). Here, the interval reciprocal to frequency range, as well as the shortened one predicted by the sampling localization theorem is also shown.

Within the retardation time interval reciprocal to the frequency range, both parameters  $E$  and  $S$  oscillate between some maximum and minimum values and the parameters vary in “anti-phase”, i.e. error minimums are related to maximums of noise gain, and vice versa. Out of the reciprocal frequency range, both the parameters grow. The filters of the bank have relatively low noise gains with mean value  $\bar{S} = 3.26$  for all the filters and  $\bar{S} = 2.47$  – for the filters within the reciprocal frequency range.

## 6 Conclusions

The inherent drawbacks of filtering algorithms used for recovering the relaxation and retardation spectrum (RRS) have been identified, such as (i) exponential shortening intervals of relaxation/retardation time due to the end effects of discrete convolution algorithms for geometrically sampled

datasets, (ii) rare spectrum points due to relatively large progression ratios have to be used to keep noise amplification at acceptably low levels, (iii) inconvenience of finite decimal (non-integer) progression ratios requiring resembling input data.

To overcome the mentioned drawbacks, construction of RRS recovery algorithms has been proposed by uniting asymmetric filters with shifted origins (zero points) of impulse responses.

A filter bank composed of 25 filters has been developed, which from the real part of complex compliance recorded at frequencies spaced geometrically with progression ratio 2 recovers the retardation spectrum with doubled sampling density over the time interval  $0.5\omega_{\max}^{-1} < \tau < 2\omega_{\min}^{-1}$

## Acknowledgements

This work was supported by the European Regional Development Fund (ERDF) under project No. 2010/0213/2DP/2.1.1.1.0/10/APIA/VIAA/017.

## References:

- [1] J.D. Ferry, *Viscoelastic Properties of Polymers*, 3rd. ed., J. Wiley and Sons, 1980.
- [2] N.W. Tschoegl, *The Phenomenological Theory of Linear Viscoelastic Behavior*; Springer-Verlag, 1989.
- [3] N.G. McCrum, B.E. Read, G. Williams, *Anelastic and Dielectric Effects in Polymer Solids*, J. Wiley and Sons, 1967.
- [4] A.K. Jonscher, *Dielectric Relaxation in Solids*, Chelsea Dielectric, 1983.
- [5] F. Kremer, A. Schonhals, W. Luck, *Broadband Dielectric Spectroscopy*; Springer-Verlag, 2002.
- [6] C.P. Slichter, *Principles of Magnetic Resonance*; 3rd. enlarged and updated ed., Springer-Verlag, 1996.
- [7] J.R. Macdonald, Comparison of parametric and nonparametric methods for the analysis and inversion of immittance data: Critique of earlier work, *J. Comp. Phys.*, Vol. 157, 2000, pp. 280-301.
- [8] J.R. Macdonald, E. Tuncer, Deconvolution of immittance data: Some old and new methods, *J. Electroanalytical Chem.*, Vol. 602, 2007, pp. 255-262.
- [9] A.V. Oppenheim, R.V. Schaffer, *Discrete-Time Signal Processing*, Sec. Ed., Prentice-Hall International, 1999.
- [10] S.W. Smith, *The Scientist and Engineer's Guide to Digital Signal Processing*, 2<sup>nd</sup>, California Technical Publishing, 1999.
- [11] V. Shtrauss, Digital interconversion between linear rheologic and viscoelastic material functions. In: *Advances in Engineering Research*. Vol. 3, Ed. V.M. Petrova, Nova Science Publishers, 2012, pp. 91-170.
- [12] V. Shtrauss, Determination of the relaxation and retardation spectra – A view from the up-to-date signal processing perspective, *Mech. Comp. Mat.*, Vol. 48, 2012, pp. 27-46.
- [13] V. Shtrauss, Determination of relaxation and retardation spectrum by inverse functional filtering, *J. Non-Newtonian Fluid Mech.*, Vol. 165, 2010, pp. 453-465.
- [14] V. Shtrauss, A user-oriented approach to designing FIR deconvolution filters, *Proc. 12th WSEAS International Conference on Systems Theory and Scientific Computation*, Advances in Systems Theory, Signal Processing & Computational Science, Istanbul, Turkey, August 21-23, 2012, pp. 130-135.
- [15] V. Shtrauss, Sampling and algorithm design for relaxation data conversion, *WSEAS Transactions on Signal Processing*, Vol. 2, 2006, pp. 984-990.
- [16] V. Shtrauss, Decomposition of multi-exponential and related signals – Functional filtering approach, *WSEAS Transactions on Signal Processing*, Vol. 4, 2008, pp. 44-52.
- [17] A. Kalpinsh, V. Shtrauss, Measurement systems for distribution of relaxation and retardation times, *Proc. 15th WSEAS International Conference on Systems RECENT RESEARCHES in SYSTEM SCIENCE*, Corfu Island, Greece, July 14-16, 2011, pp. 106-111.
- [18] K.S. Cole, R.H. Cole, Dispersion and absorption in dielectric. Alternating current characteristics, *J. Chem. Phys.*, Vol. 9, 1941, pp. 341-351.
- [19] A. Arguez, P. Yu, J.J. O'Brien, A new method for time series filtering near endpoints, *J. Atmos. Oceanic Tech.*, Vol. 25, 2008, pp. 534-546.
- [20] V. Shtrauss, Spectrum analysis and synthesis of relaxation signals, *Signal Processing*, Vol. 63, 1997, pp. 107-119.
- [21] V. Shtrauss, FIR Kramers-Kronig transformers for relaxation data conversion, *Signal Processing*, Vol. 86, 2006, pp. 2887-2900.
- [22] A.R. Davies, R.S. Anderssen, Sampling localization in determining the relaxation spectrum, *J. Non-Newtonian Fluid Mech.*, Vol. 73, 1997, pp. 163-179.
- [23] M. Renardy, On the use of Laplace transform inversion for reconstruction of relaxation spectra, *J. Non-Newtonian Fluid Mech.*, Vol. 154, 2008, pp. 47-51.